Journal of Neuromuscular Diseases 1 (2014) S1–S7
IOS Press

Research Report

Mutations in the Mitochondrial Citrate Carrier SLC25A1 are Associated with Impaired Neuromuscular Transmission

Amina Chaouch[a], Vito Porcelli[b], Daniel Cox[a], Shimon Edvardson[c], Pasquale Scarcia[b], Anna De Grassi[b], Ciro L. Pierri[b], Judith Cossins[d], Steven H. Laval[a], Helen Griffin[a], Juliane S. Müller[a], Teresinha Evangelista[a], Ana Töpf[a], Angela Abicht[e,f], Angela Huebner[g], Maja von der Hagen[g], Kate Bushby[a], Volker Straub[a], Rita Horvath[a], Orly Elpeleg[c], Jacqueline Palace[h], Jan Senderek[f], David Beeson[d], Luigi Palmieri[b,i] and Hanns Lochmüller[a,*]

[a]*Institute of Genetic Medicine, MRC Centre for Neuromuscular Diseases, Newcastle University, Newcastle upon Tyne, UK*
[b]*Department of Biosciences, Biotechnology and Biopharmaceutics, University of Bari Aldo Moro, Bari, Italy*
[c]*Monique and Jacques Roboh Department of Genetic Research, Hadassah, Hebrew University Medical Center, Jerusalem, Israel*
[d]*Neurosciences Group, Nuffield Department of Clinical Neurosciences, University of Oxford, John Radcliffe Hospital, Headley Way, Oxford, UK*
[e]*Medizinisch Genetisches Zentrum, Munich, Germany*
[f]*Friedrich-Baur-Institut, Ludwig Maximilians University, Munich, Germany*
[g]*Children's Hospital, Technical University Dresden, Dresden, Germany*
[h]*Department of Clinical Neurology, The John Radcliffe, Oxford, UK*
[i]*CNR Institute of Biomembranes and Bioenergetics, Bari, Italy*

SUPPLEMENTARY VIDEO

Video footage of 48hpf zebrafish embryos following co-injection of SLC25A1a (5 ng) and SLC25A1b (2.5 ng): Mildly (Top Right), moderately (Bottom Left), and severely (Bottom Right) affected embryos demonstrate a reduced heart rate compared to that of the non-injected Wild Type Golden control embryos (Top Left)".

*Correspondence to: Hanns Lochmüller, Institute of Genetic Medicine, International Centre for Life, Newcastle University, Newcastle upon Tyne, NE1 3BZ, UK. Tel.: +44 191 2418602; Fax: +44 191 2418770; E-mail: hanns.lochmuller@ncl.ac.uk.

SUPPLEMENTARY MATERIAL

Materials and methods

Exome sequencing

DNA library preparation and whole-exome sequencing were outsourced to EuroFins MWG Operon (Germany). Sequencing was achieved using Agilent SureSelect capture and Illumina HiSeq2000 (2×100bp reads) sequencing platforms. Raw sequencing data were aligned to the human reference genome (hg19), sorted and converted to a BAM file using bwa. The BAM file was indexed and variants called using SAMtools (version 0.1.16) [38]. The

ISSN 2214-3599/14/$27.50

alignments were optimised for indel calling using dindel (version 1.0.12) [39]. Variants called were annotated using ANNOVAR [40]. The filtering algorithm was applied to exclude non-coding, frequent variants calls (mean allele frequency (MAF)>1%) found in public databases of single nucleotide polymorphisms (SNP) (dbSNP [http://www.ncbi.nlm.nih.gov/SNP/], the Exome Variant Server [http://evs.gs.washington.edu/EVS/], the 1000 Genomes Project [http://www.1000genomes.org]) and an in house list of common variants from unrelated controls.

Variants were visualised and evaluated using the UCSC Genome Browser, [41]. Sanger sequencing was used to verify putative disease-causing variants and their segregation with the disease. All primer sequences used are available on request. Sanger sequencing was performed using bi-directional fluorescent sequencing on an ABI 3730 XL 96 capillary sequencer, with BigDye Version 3.1 chemistry (Life Technologies®). The GenBank reference number NM_005984 was used as reference for the mRNA sequence of *SLC25A1*.

STRUCTURAL ANALYSIS OF SLC25A1 PATHOGENIC MUTATIONS

Materials and methods

Modeller [42] was used to calculate three dimensional structural models of human CIC R247Q mutant using the structure of the bovine BtAAC1 (protein data bank accession code: 1okc (43) as template for the comparative modelling (see also [17]). For docking analysis, citrate ligand was docked into the predicted binding site using Autodock 1.5.2.1 [44]; for citrate docking see also [17]).

RESULTS

R247 is located at the end of transmembrane helix 5 (Supplementary Figure 2b) in correspondence of the second highly conserved basic residue of the first part of MC sequence motif (Px[D/E]xx[K/R]x[R/K]). R247 forms ionic interactions with the acidic residue E270, which is located at the end of the short helix h56 parallel to the membrane plane in correspondence of the highly conserved acidic residue of the second part of MC sequence motif ([D/E]GxxxxAr[R/K]G). R247 replacement with the shorter/uncharged glutamine affects the local ion-pair network and related conformational changes due to the putative newly established weaker hydrogen (water mediated) bonds with E270.

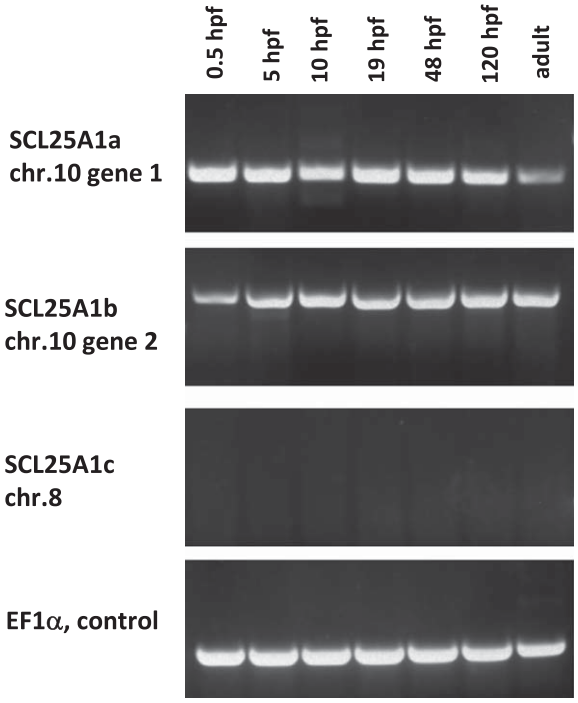

Supplementary Figure 1. RT-PCR analysis of SLC25A1 orthologs at different stages of zebrafish development. Both SLC25A1 genes on Chr.10 (SLC25A1a & SLC25A1b) are expressed from 0.5 hours post fertilisation (hpf) and maintained throughout development into adulthood. SLC25A1 gene on Chr.8 is not expressed during zebrafish development or adulthood. EF1α: elongation factor 1 alpha was used as internal RT-PCR control for all time points to certify cDNA synthesis quality.

DISCUSSION

All mitochondrial carrier family members have common structural features; their primary structures consist of three tandemly repeated homologous domains of approximately 100 residues in length, and each repeat contains two hydrophobic segments and a characteristic sequence motif Px[D/E]xx[K/R]x[R/K] (20-30 residues) [D/E]GxxxxAr[R/K]G. In 2003 the structure of a member of the mitochondrial carrier family, the ADP/ATP carrier, was determined [29]. Based on the strikingly conserved repeats organization and primary structure it is assumed that all the members of the mitochondrial carrier family share a common overall structure consisting of a six-transmembrane a-helix (H1-H6) bundle and three short α-helices (h12, h34 and h56) parallel to the membrane plane on the matrix side [45]. Mitochondrial carriers (MCs) possess

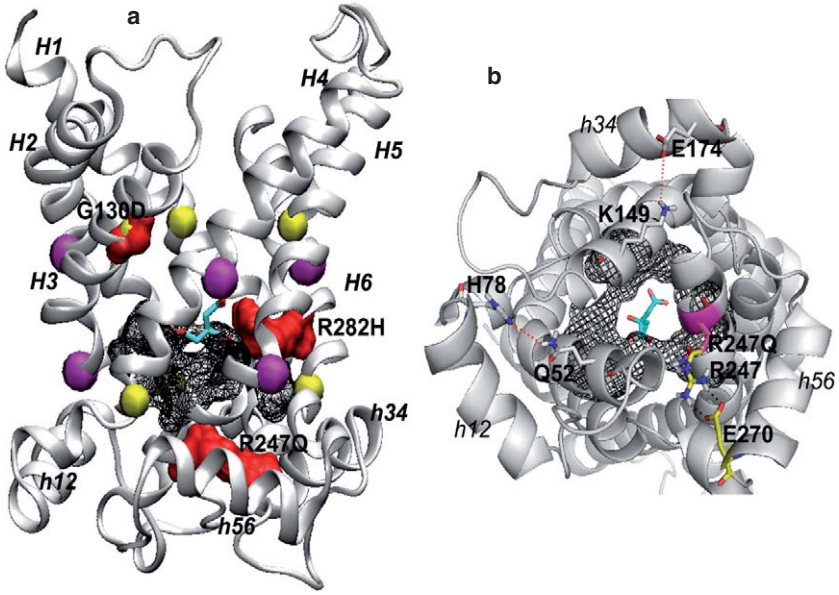

Supplementary Figure 2. Structural comparative model of human CIC and docking of citrate. The 3D comparative model of human CIC is reported in white cartoon representation. The six transmembrane helices are indicated by black labels (H1-H6). The three short helices parallel to the membrane planes are also labelled (h12, h34, and h56). The citrate ligand is shown in cyan licorice. The residues forming the m-gate are reported in black mesh representation. Panel (A): lateral view of the human citrate carrier. Prolines (magenta beads) and glycines (yellow beads) of the PG levels (or the corresponding residues) surround the substrate binding area. The pathogenic mutations R247Q (this work), G130D and R282H are reported in red surf representation and are indicated by black labels. Panel (B): Bottom view of the 3D comparative model of human CIC. The pathogenic mutation R247Q is reported in magenta licorice representation. R247 and E270 are reported in yellow sticks representation. Black dashed lines indicate ionic bonds (both shorter than 2.5 Å). The symmetrical interactions observed on the first and on the second repeat (K174-E149 and Q52-H78, shown in white sticks representation) are also reported for comparative purposes. Red dashed lines indicate putative (water mediated) H-bond interactions (among 5.5 and 6.5 Å).

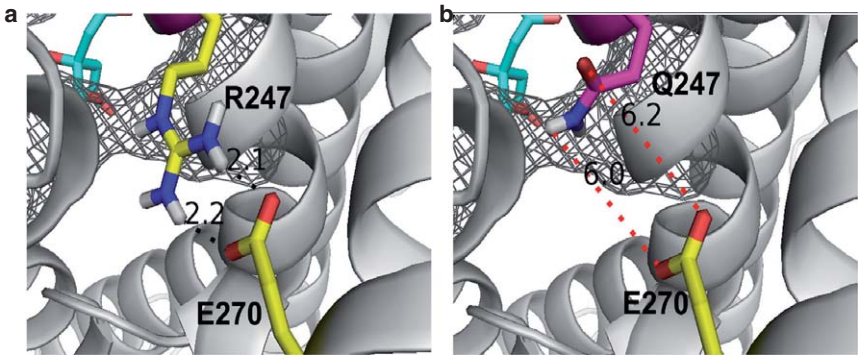

Supplementary Figure 3. Exploded view of the salt bridge between R247 and E270 (panel A) and of the putative H-bond interactions between Q247 and E270 (panel B). Colours and graphical representations as in Supplementary Figure 2.

a funnel-shaped central cavity, lined by the six transmembrane helices, and two gates (the matrix gate (m-gate) and the cytosolic-gate (c-gate)) alternately open on the cytosolic or the matrix side [30, 46]. As the substrate binds to the carrier in the conformation open towards the cytosol, the protein rearranges until the transition state is reached in agreement with the "induced transition fit" [30, 47] of carrier catalysis. In the transition state the substrate is bound at the centre of the carrier to residues located at the level of the proposed common binding site [48]. The substrate binding in the transition state triggers additional structural changes, hinged on two sets of proline-glycine residues (Supplementary Figure 2a), forming the so called PG levels [30], leading to the opening of the carrier on the matrix side and to the closure of the

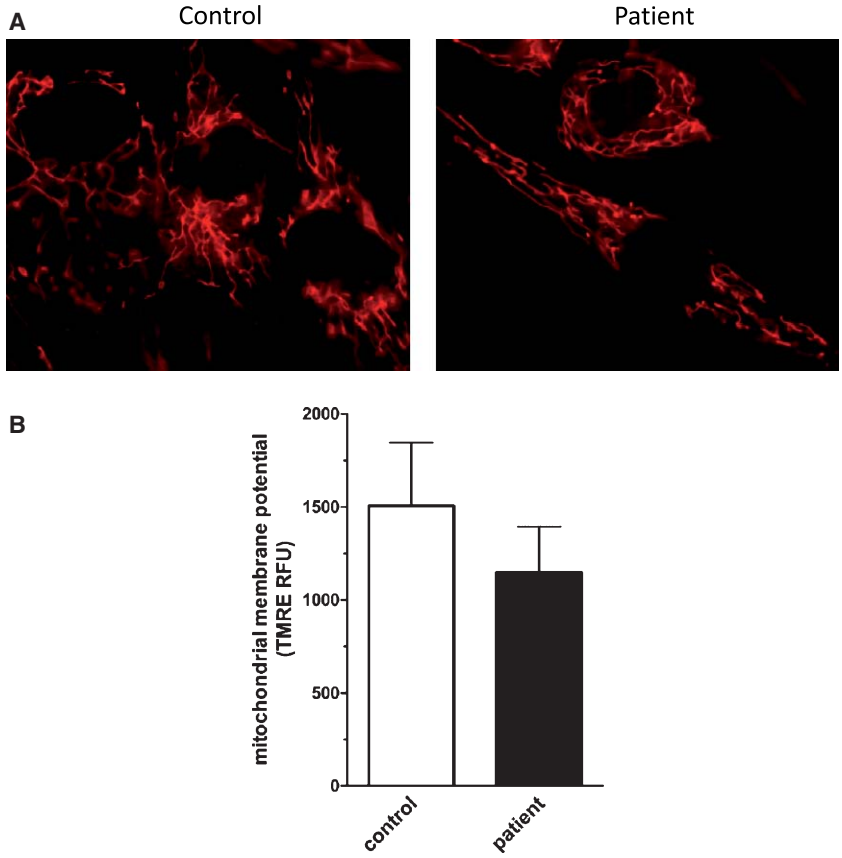

Supplementary Figure 4. Mitochondrial staining in fibroblast cells relative to control and patient (panel A). Mitochondrial Staining with Mitotracker Mitochondrion-selective Probes- Medium containing Mitotracker Red CMXRos in a range of 10–500 nM was added to cells grown on tissue culture chamber slides and incubated at 37°C for 30–45 min. After incubation, the medium containing the Mitotracker dye was replaced with fresh medium, and the stained cells were observed by fluorescence microscopy. The same cells were used to measure mitochondrial membrane potential using the tetramethylrhodamine methyl ester (TMRM) probe. $\Delta\Psi$ measured as relative fluorescence units (RFU) is presented as mean $\pm$ SD of three experiments (panel B).

carrier on the cytosolic side. At this stage the substrate (which entered the carrier from the cytosolic side) exits into the matrix and the cycle continues with the entry of another substrate from the matrix. During the transition from the cytosolic conformation to the matrix conformation, charged residues [25], located just below the matrix gate. Residues of the matrix gate area are involved in crucial intra-/inter-repeat interactions [49] that allow efficient conformational changes for the substrate translocation. The charged residues of the human citrate carrier m-gate area mainly involved in the above cited conformational changes, allowing an efficient citrate translocation are R247, E270, Q52, H78, K149 and E174 (Fig. 1B). All these residues protrude into the mitochondrial matrix.

Previously characterized mutations R282H and G130D concerned residues R282 and G130 located at the substrate binding site and at the PG level 1, respectively. More in detail R282 is located in transmembrane helix 5, three residues below the contact point III of the putative common substrate binding site of the mitochondrial carrier family (see Fig. 2B of [17]). Its position together with the observation that R282 is not conserved in other mitochondrial carriers suggests a role in substrate specificity. G130 is located in transmembrane helix 3 at the PG level 1 (see Fig. 2B of [17]), a mitochondrial carrier region involved in conformational changes occurring during the translocation mechanism, and is also conserved in several other mitochondrial carriers (Fig. 2A of [17]).

In the mutated R282H protein, the substrate cannot reach the proposed binding site on the bottom of the carrier cavity and is trapped at the level of K97 (see Fig. 3C of [17]) abolishing completely citrate transport.

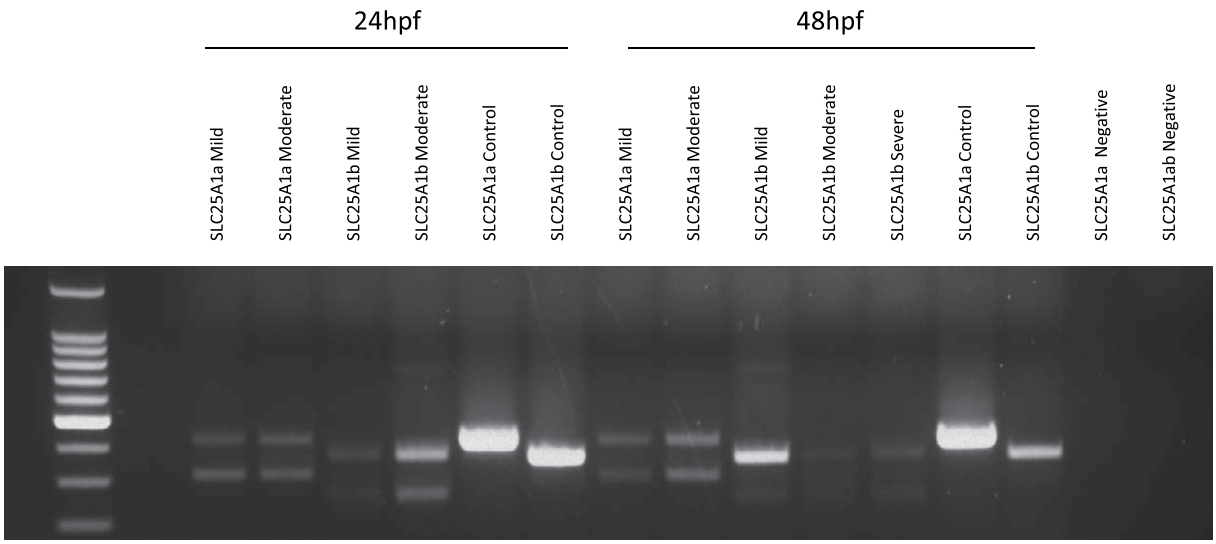

Supplementary Figure 5. RT-PCR analysis of SLC25A1a and SLC25A1b MO induced phenotypes at different stages of zebrafish development. Both SLC25A1a & SLC25A1b induce splicing of the associated genes on Chr.10 at both 24hpf and 48hpf.

In the G130D protein (Fig. 3B of [17]), the binding site is apparently unaffected. However, the mutation leads to the replacement of the small neutral amino acid glycine with the bulkier negatively charged aspartic acid which protrudes towards transmembrane helix 4, introducing an important perturbation of local secondary structures that affects quite severely conformational changes hinged on residues of the PG level 1

At variance with the previous described mutations, R247 is located immediately below the m-gate, quite distant from the proposed common binding site and from PG levels. R247 forms an intra-repeat salt bridge with E270. In our patient R247 is replaced by the shorter/uncharged glutamine residue. This mutation results in the replacement of the ionic interaction R247-E270 with the putative H-bond (water-mediated) weaker interaction Q247-E270 (Supplementary Figure 3). It can be speculated that this mutation affects conformational changes and substrate translocation without altering citrate affinity (at variance with R282H) and more in general less severely than G130D. Notably, a glutamine residue in place of a basic (R/K) residue is often found at the end of the first part of MC sequence motif [25] and it is also detected in the first repeat of citrate carriers (Q52, see Supplementary Figure 2).

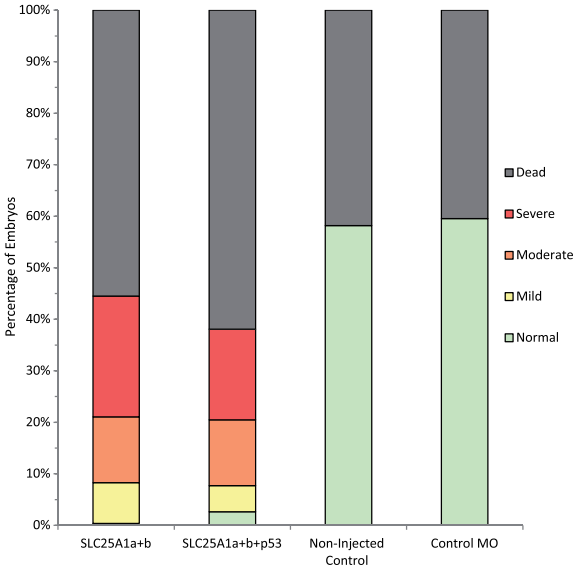

Supplementary Figure 6. Percentage of phenotypes observed in zebrafish following injection of SLC25A1a+b MO in the presence and absence of anti-p53 MO compared to non-injected control and control MO injected embryos. Non-injected control embryos and those injected with a standard control MO showed similar percentage of survival. Combined SLC25A1 MO with and without the addition of anti-p53 MO demonstrate reduced percentage of survival. Co-injection with anti-p53 MO displays a reduced percentage of severe phenotypes observed.

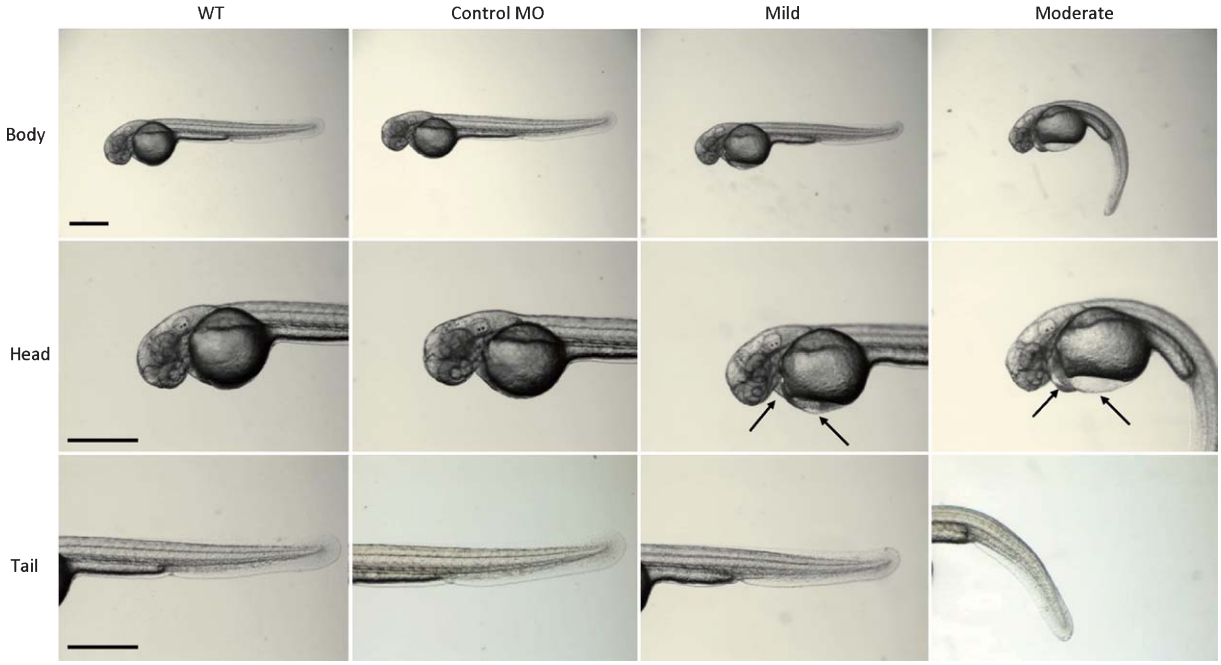

Supplementary Figure 7. Morphology of 48hpf SLC25A1 morphant embryos. Live embryos imaged at 48hpf following co-injection of SLC25A1a (5 ng), SLC25A1b (2.5 ng) and anti-p53 MO. Embryos were injected with an anti-p53 MO, suppressing the non-specific MO mediated apoptotic affects produced by p53 activation. Injected embryos also demonstrated a range of phenotypes from mildly to severely affected. Embryos exhibit a developmental delay with curvature and shortening of the tail and also oedema of the hindbrain, heart, yolk sac and tail. Scale bars: 500 μm.

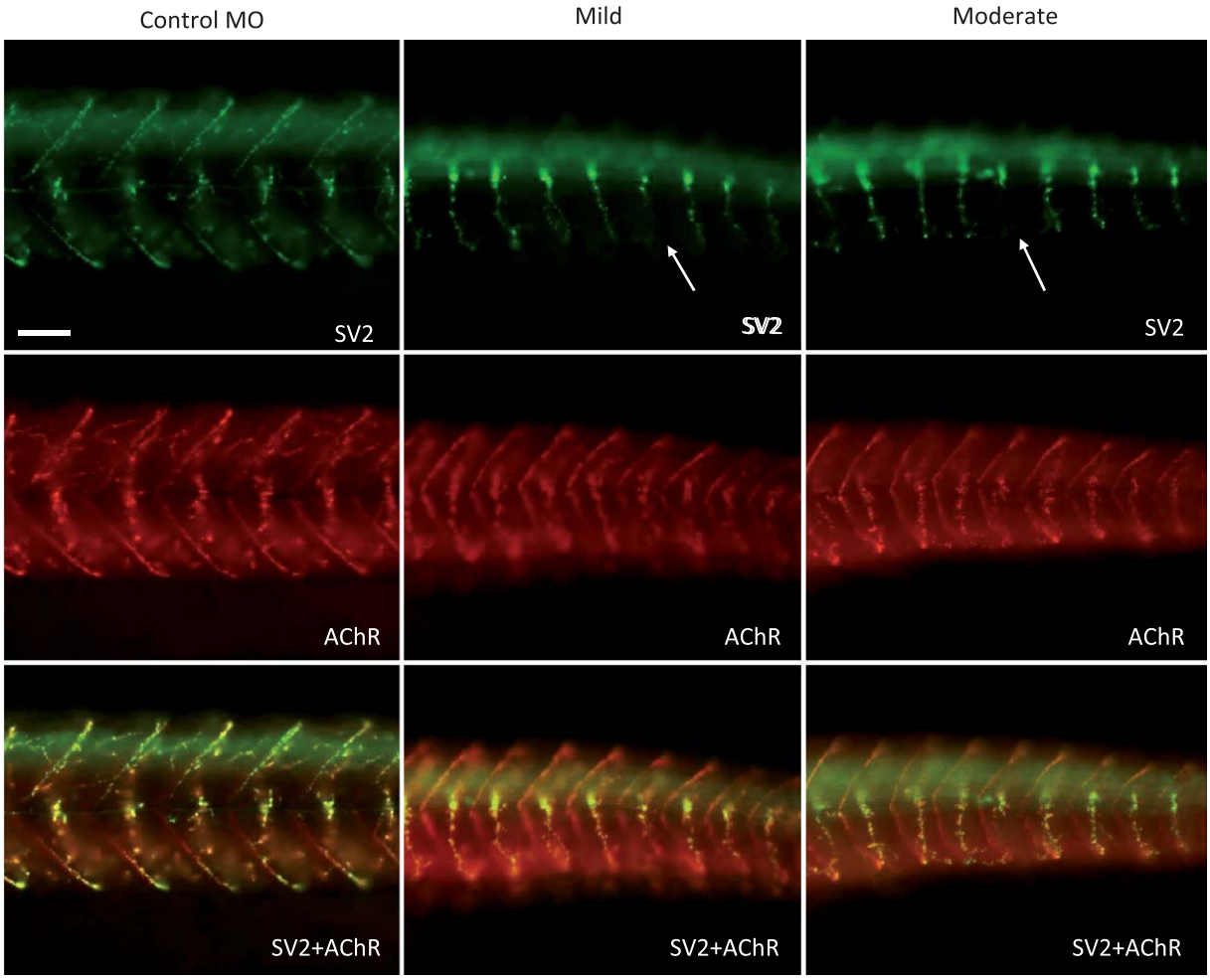

Supplementary Figure 8. Neuromuscular junctions following injection with SLC25A1 MOs and anti-p53 MO. Embryos injected with a standard control MO showed no signs of neuronal abnormality and were indistinguishable from non-injected wild type embryos. WilSLC25A1 MO injected embryos (centre and right) were stained for postsynaptic AChR (α-bungarotoxin, red staining) and presynaptic nerve endings (SV2 antibody, green staining). Combined SLC25A1 MO (a 5 ng & b 2.5 ng) with the addition of anti-p53 MO injected 48hpf embryos also exhibit shortening and branching of motor axons. Scale bar: 50 μm.